Uranium Nitride as LWR TRISO Fuel: Thermodynamic Modeling of U-C-N and Thermomechanics

T. M. Besmann, D. Shin, T. B. Lindemer, M. K. Ferber, P. F. Becher, A. A. Wereszczak, and H. T. Lin
Materials Science and Technology Division
Oak Ridge National Laboratory

Introduction

A new concept for light water reactor (LWR) nuclear fuel has recently been proposed that utilizes pellets of tristructural isotropic (TRISO) fuel particles embedded in a SiC or zirconium alloy matrix, replacing sintered urania pellets [1,2]. The fuel is considered significantly more accident tolerant than urania as the SiC matrix or coated/protected zirconium alloy and TRISO particles would be highly resistant to oxidation and fission product release under beyond-design-basis accident conditions. As is well understood, failed fuel rods release gaseous and volatile fission products, and that is greatly exacerbated as urania oxidizes from UO_{2+x} to higher oxidations states in failed fuel pin with resulting expansion, loss of integrity, and significant further release of fission products.

The envisioned LWR TRISO would consist of a several hundred micrometer fuel kernel coated with sequential layers of a low density carbon (buffer layer) which serves to absorb the energy of fission recoil particles and provide a volume for released fission gas, a seal layer of high density pyrolytic carbon (inner pyrolytic carbon), a layer of SiC that adds strength and provides a barrier to fission products that escape through the carbon layer, and an outer layer of high density pyrolytic carbon (outer pyrolytic carbon) that provides for an interface layer with the matrix and improves particle strength by putting the SiC layer in compression.

One of the issues that is being addressed in the LWR TRISO concept is having sufficient fissile uranium concentration within a pellet to obtain adequate reactivity. With the actinide containing kernel in the TRISO particle occupying a fraction of the volume, and the need to distribute particles within the matrix of the pellets, the overall fissile metal content is problematic. The result is that a UO_2 kernel, or even a UO_2-UC_2 kernel, euphemistically termed "UCO," may be inadequate. Hence the renewed interest in uranium nitride fuel where UN would have a significantly higher metal atom fraction than the dioxide or dicarbide.

The SiC matrix and TRISO fuel particles are expected to be stable to high temperature oxidation in air, and the thermal conductivity of the composite fuel system will be greatly increased due to the SiC matrix. The thermal conductivity, while significantly higher, does depend upon 1) the TRISO particle content and 2) the thermal transport across the interfaces within the TRISO particles and between the particles and the SiC matrix, as well as that of the matrix. Mismatches in thermal and elastic properties exist between the TRISO particle core, the coating layers and the SiC matrix. These property mismatches will introduce stresses within the various components during the heating/cooling cycles experienced during fuel processing and during normal reactor cycles. As a result, thermomechanics modeling studies were initiated to examine the factors that influence the generation of stresses and the fuel performance.

Thermochemical Behavior of U-C-N

The preparation of UN by the carbothermic reduction of urania followed by nitriding, and the intimate contact of a UN TRISO kernel with the carbon of the buffer layer is the reason for the current interest in the U-C-N system. The U(C,N) phase is stable as the UC and UN phases are isostructural (NaCl structure) and have been observed to form a complete solid solution [3-10]. Austin and Gerds [3], Henry and Blickensderfer [6], Leitnaker et al. [9], and Cordfunke and Ouweltjes [10] provide at least partial ternary U-C-N phase diagrams, with the latter computing a diagram at 1968K assuming a simple ideal solution between UC and UN. Henry and Blickensderfer [6] provide a detailed diagram at 1973K from compositional observations which provide for a small homogeneity range for both UC and UN, yet otherwise largely agree with Cordfunke and Ouweltjes [10], and Leitnaker et al.[9].

Vapor/dissociation pressure measurements have been made in U(C,N)-containing systems by Sano et al [5], Ikeda et al [8], Cordfunke and Ouweltjes [10], and Prins et al [11]. Leitnaker [4] using an inverse approach determined lattice parameters for the solid solution where UC reacted with nitrogen and UN reacted with carbon.

The reported measurements with respect to U(C,N) are reviewed and used in the current study to determine a solid solution representation of the phase. The model for the phase together with free energies for the elemental and binary phases are in turn used to derive high temperature ternary U-C-N phase diagrams. Equilibrium nitrogen pressures have been computed for conditions of interest for fabrication and in-reactor behavior of U(C,N) LWR TRISO fuel.

Thermochemical Data

Free energies for phases in the U-C system were obtained from the assessment of Chevalier and Fischer [12] and similarly for the U-N system from Chevalier et al. [13]. While values for the relevant phases and species in the U-C-N system are reported in established tables, the comprehensive nature of the above assessments encouraged their use in the current work. The UN phase, while reported to have a compositional range from stoichiometric to slightly hypostoichiometric, was treated as the line compound, UN. The sesquinitride phase values were adopted from Chevalier et al. [13] with the stoichiometry of $U_{2.065}N_{2.935}$, termed "U_2N_3." According to the assessment, the assumption is relatively accurate at higher temperatures. Elemental phase and gaseous species data were also taken from of Chevalier and Fischer [12] and Chevalier et al. [13], and were noted to be consistent with those from both the FactSage [14] and JANAF Thermochemical Tables [15] databases, and which were used to provide values for the minor species. Table 1 summarizes the Gibbs free energy values used in the calculations for the condensed phases and N_2 and U gaseous species.

Table 1. Gibbs free energy expressions for constituents used in thermochemical modeling of the U-C-N system after Chevalier and Fischer [12] and Chevalier et al. [13].

$G = a + bT + c\,T \ln(T) + d\,T^2 + e\,T^3 + f\,T^{-1} + g\,T^{-2} + h\,T^{-3}$ (J/mol)

	a	b	c	d	e	f	g	h
N_2 gas	-1.98800E+04	6.11431E+01	-3.62147E+01	-3.00594E-04	8.00304E-09	2.51099E+06		
U gas	5.40141E+05	-2.01813E+02	-1.44474E+00	-9.05920E-03	1.17787E-07	-2.69701E+06		
U liquid	-1.01663E+04	2.81797E+02	-4.86600E+01					
C (graphite)	-1.73684E+04	1.70300E+02	-2.43000E+01	-4.72300E-04		2.56260E+06	-2.64300E+08	1.20000E+10
UC	-1.17760E+05	3.43906E+02	-5.95212E+01	1.14276E-04	-6.48440E-07	4.35560E+05		
U_2C_3	-2.44460E+05	8.75767E+02	-1.50061E+02	2.33936E-02	-6.81765E-06	1.44483E+06		
UC_2								

-1.31112E+05 6.37772E+02 -1.04889E+02 2.56127E-02 -5.49663E-06 1.61471E+06 -2.64300E+07 1.20000E+09

UN*

-3.01531E+05 3.14074E+02 -5.55311E+01 -7.58320E-05 -7.76780E-07 3.83756E+05

“U_2N_3”**

-7.42499E+05 8.64747E+02 -1.46391E+02 -4.14249E-03 -2.26010E-06 2.08770E+06 -2.38295E+05

*Gibbs free energy adjusted to by +12 kJ/mol with respect to the value of Chevalier et al. [13].
** Gibbs free energy adjusted to by +17 kJ/mol with respect to the value of Chevalier et al. [13].

The values of the free energy expression for UN of Chevalier et al. [13] and in the FactSage [14] and JANAF Thermochemical Tables [15] databases agree closely, however they all yield calculated nitrogen decomposition pressures that are significantly lower than almost all reported measurements. Figure 1 illustrates the disagreement between computed and measured values. This discrepancy also extends to measurements of nitrogen decomposition pressures measured over U(C,N) when an ideal solution model is used to represent the phase, as detailed below. An effort was thus made to adjust the thermodynamic values for UN to obtain better agreement with nitrogen pressure data. (Note that considering the non-stoichiometry of UN would increase the discrepancy as hypostoichiometric UN would be computed to have an even lower nitrogen decomposition pressure.) The adjustment of the UN Gibbs free energy by +12 kJ/mol from that of Chevalier et al. [13], an equivalent 298K heat of formation of -282.3526 kJ/mol, appears to bring the computed pressures into relative agreement with reported measurements (Fig. 1), and the resultant free energy values for UN will be used in representing U(C,N). This adjusted value is near the lower, more positive bound of the range of third law heats of formation from analysis of the pressure measurements given in Fig. 1, reported to extend from -276 to -296 kJ/mol.[8, 11, 16-21].

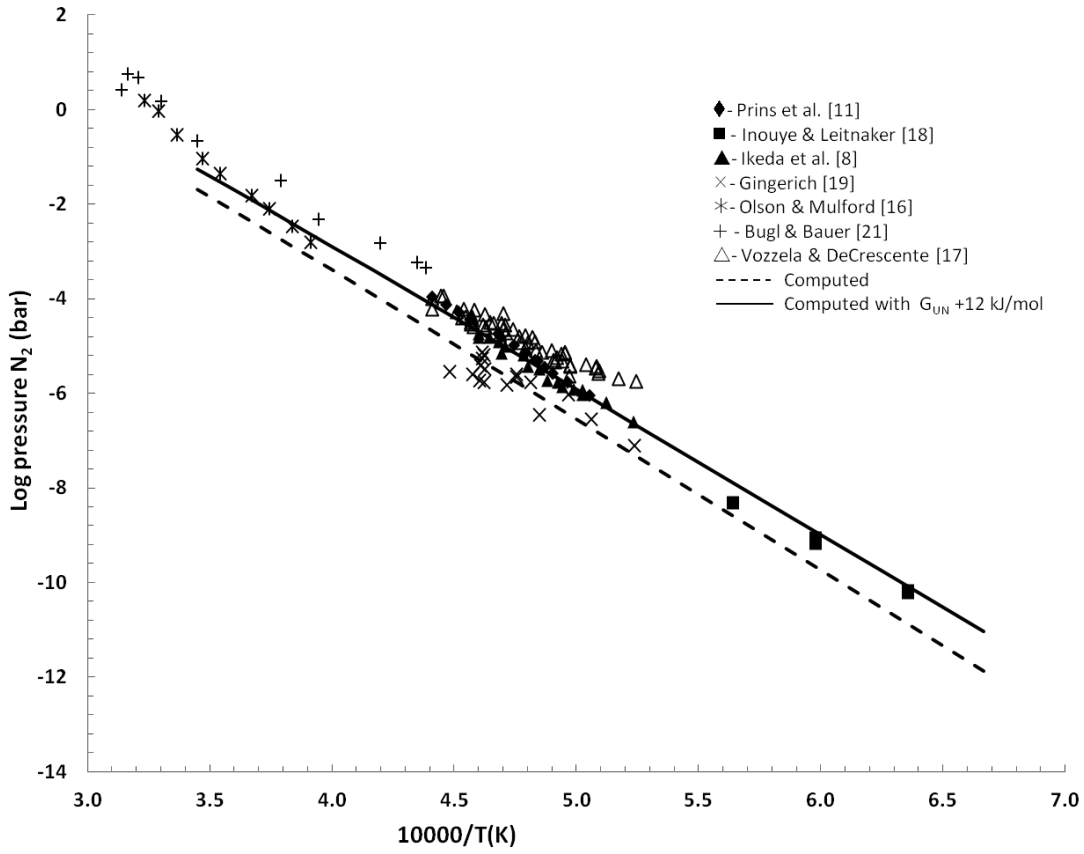

Fig. 1. Plot of reported UN decomposition nitrogen pressure versus reciprocal temperature data and computed pressures both from the values of Chevalier et al. [13] and their Gibbs free energy for UN increased by +12 kJ/mol.

Gingerich [19], Ikeda et al. [8], and Prins et al. [11] have additionally determined UN decomposition uranium pressures. These are consistently lower than would be expected in the presence of uranium liquid, which would be expected to be present at the decomposition of UN were it a line compound. This likely reflects the hypostoichiometry of the UN phase, i.e., UN_{1-y}, where the equilibrium pressures are actually measured over the single phase nitride where nitrogen loss due to the generation of a nitrogen pressure results not in uranium liquid formation but rather in a lower stoichiometry nitride. Gingerich [19] reflects this in his comment that measurements were made over $UN_{0.9}$-$UN_{0.8}$.

Equilibrium Pressures and an Ideal Solution $UC_{1-x}N_x$ Model

The U(C,N) phase was treated as a solid solution of stoichiometric UC and UN, i.e., $UC_{1-x}N_x$, although as noted above there are reported small homogeneity ranges for the end-member phases. An ideal solution was adopted with the overall free energy expression for the phase

$$G = x_{UC}G_{UC} + x_{UN}G_{UN} + RT[x_{UC}lnx_{UC} + x_{UN}lnx_{UN}] \qquad (1)$$

where x_i is the mol fraction of the UC or UN inter-dissolved end member phases, G_i is the free energy of an end member phase, R is the ideal gas law constant, and T is the absolute temperature.

The data of Ikeda et al. [8] and Prins et al. [11] who report Knudsen effusion mass spectrometric measurements of nitrogen pressures over the extensive U(C,N)-U_{liq} region, were used to assess the validity of the ideal solution model for $UC_{1-x}N_x$. The results are seen in Figs. 2 and 3 with the computed pressures reasonably agreeing with the experimental measurements for all but the lowest nitrogen content samples. Prins et al. [11] determined activities from their data of UC and UN in the solid solution and also concluded that they from an almost ideal solution. Attempts to improve the fit of the data by determining interaction parameters in the Redlich-Kister formalism utilizing the optimization module within FactSage [14] were unsuccessful, yielding relatively small values that provided minimal improvement to the fit. In addition, the values were positive under some conditions, resulting in a miscibility gap for the solid solution that is not reported in phase equilibria studies. An expression for the nitrogen pressures using the ideal solution model can be determined from the reaction

$$2[UN]_{UC} = 2U_{liq} + N_2. \quad (2)$$

The free energy change from the reaction using values in Table 1 yields

$$G_{rxn} = 5.62850E+05 - 3.41101\ T - 22.4725\ T\ ln\ (T) - 1.48930E-04\ T^2 + 1.56156E-06\ T^3 + 1.74348E+06\ T^{-1}\ (J/mol). \quad (3)$$

The resulting expression for the equilibrium nitrogen pressure from the reaction of Eq. 2 and the ideal solution relations of Eq. 1 is

$$pN_2 = x^2 e^{-G_{rxn}/RT}. \quad (4)$$

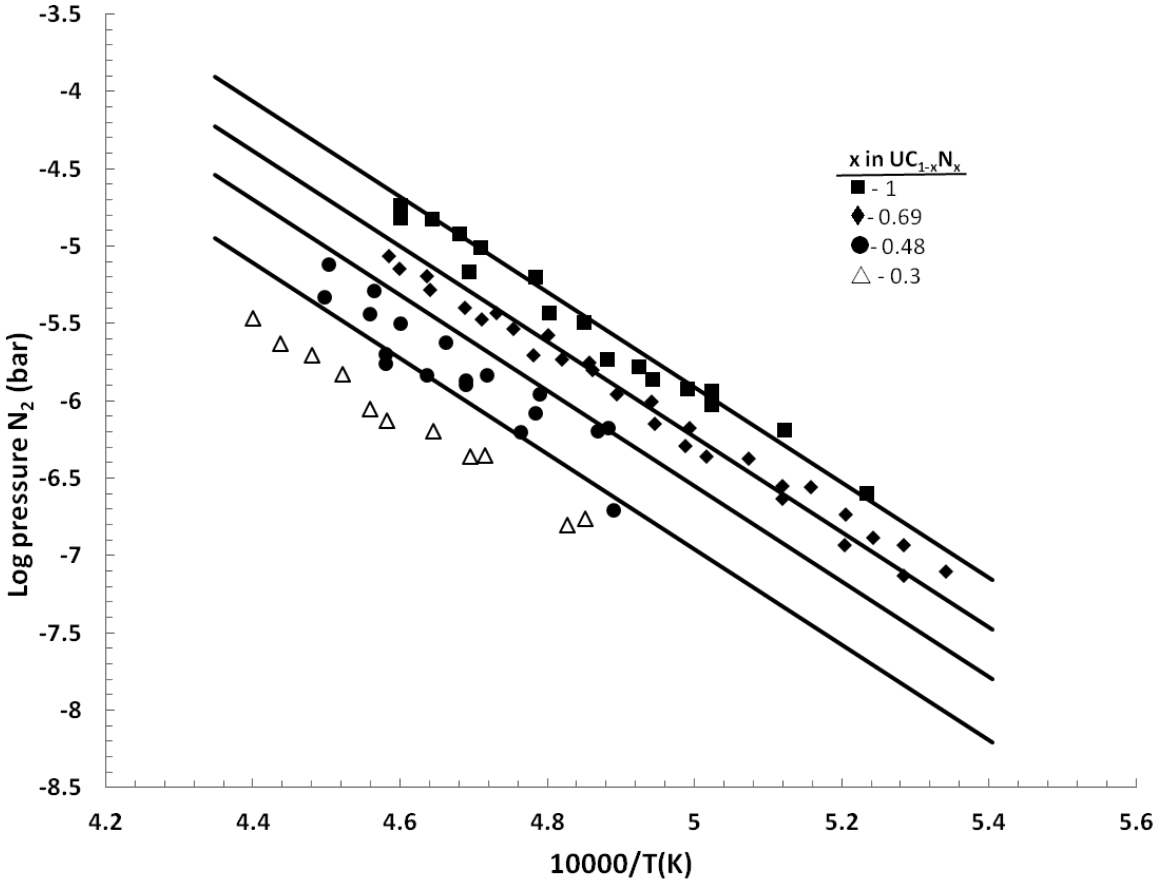

Fig. 2. Log of measured nitrogen pressures over $UC_{1-x}N_x$-U_{liq} versus reciprocal temperature for values of x determined by Ikeda et al. [8] and computed values (lines) from the ideal solid solution model for $UC_{1-x}N_x$.

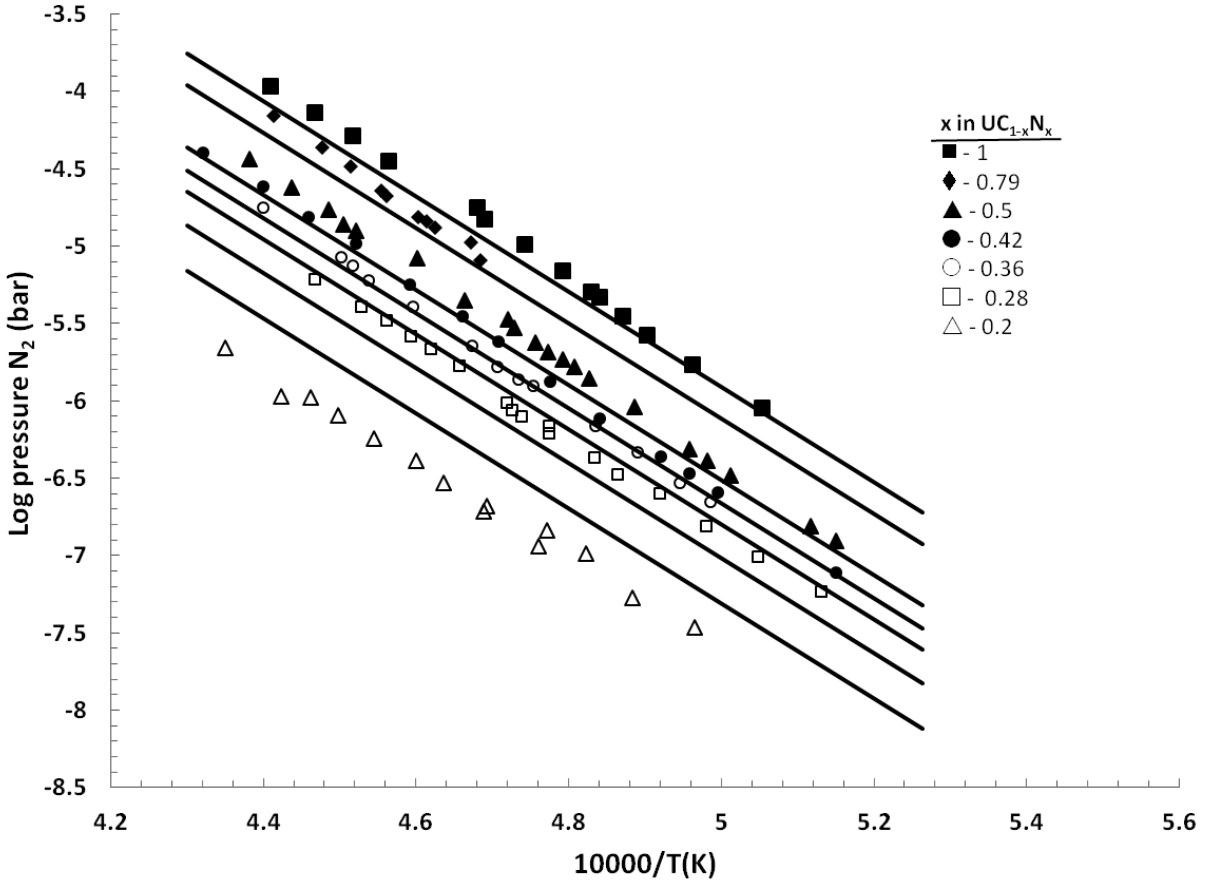

Fig. 3. Log of measured nitrogen pressures over $UC_{1-x}N_x$-U_{liq} versus reciprocal temperature for values of x determined by Prins et al. [11] and computed values (lines) from the ideal solid solution model for $UC_{1-x}N_x$.

Cordfunke and Ouweltjes [9], of the same group as Prins et al. [11], also reported nitrogen pressure measurements from off-gas analysis in the U(C,N)-C region, however they indicate oxygen present in the U(C,N) phase, although provide no determination of the amount. Leitnaker [4] reported nitrogen pressures as a function of composition during the nitriding of UC, however he indicates discrepancies with compositional analyses. In addition, the results are over a relatively narrow compositional range with approximately only a half an order of magnitude change in measured pressures. Naoumidis [7] and Naoumidis and Stoecker [22] reported pressure measurements over U(C,N)-C as a function of temperature and U(C,N) lattice parameters as well and there are limited values from Sano et al. [5]. Computed nitrogen pressures for the $UC_{1-x}N_x$ solution model equilibrated with carbon or carbides are compared with the measurements of Naoumidis and Stoecker [22] and are plotted in Fig. 4, however agreement between them is poor. An effort to determine possible interaction parameters using the Redlich-Kister formalism was unsuccessful, with optimizations in the FactSage code [14] failing to converge.

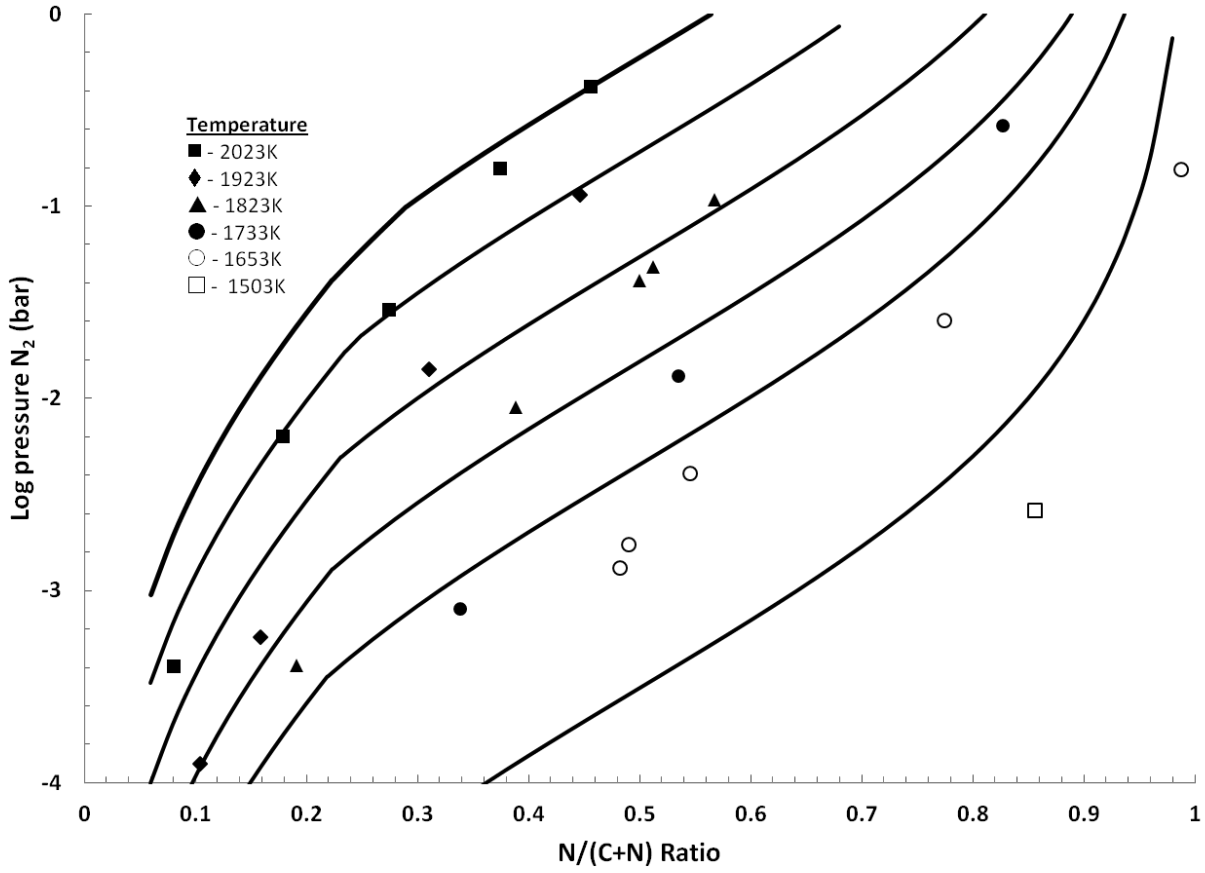

Fig. 4. Log of nitrogen pressure versus N/(C+N) ratio data for $UC_{1-x}N_x$-C or uranium carbides of Naoumidis and Stoecker [22] and computed values (lines) from the ideal solution model for $UC_{1-x}N_x$.

Computed U-C-N Phase Equilibria

Utilizing the thermodynamic values noted above and the ideal solution representation of the $UC_{1-x}N_x$ phase, isothermal sections of the ternary U-C-N phase diagram were computed using the Thermocalc software [23] assuming 1 bar total pressure. Initial computed diagrams indicated that the "U_2N_3" phase was stable to high temperatures, whereas the assessed diagram of Chevalier et al. [13] and others indicate the sesquinitride is stable only below ~1600K. This is apparently an artifact from reducing the stability of UN by 12 kJ/mol in order to improve the fit of the nitrogen pressure data. To obtain consistency with known phase equilibria, it was necessary to make the Gibbs free energy of the"U_2N_3" phase more positive by 17 kJ/mol than that of Chevalier et al. [13] in order to obtain its relative stability limit at ~1600K. The resulting computed diagram at 1973K is seen in Fig. 5. While there is an extensive two-phase region for $UC_{1-x}N_x$-U_{liq} that spans the entire UC-UN join, regions at higher carbon and nitrogen contents have multiple equilibria with $UC_{1-x}N_x$. At this temperature both U_2C_3 and UC_2 are stable and form regions with $UC_{1-x}N_x$ as does carbon and nitrogen. At lower temperatures UC_2 is no longer stable, as reflected in the 1500K computed diagram of Fig. 6.

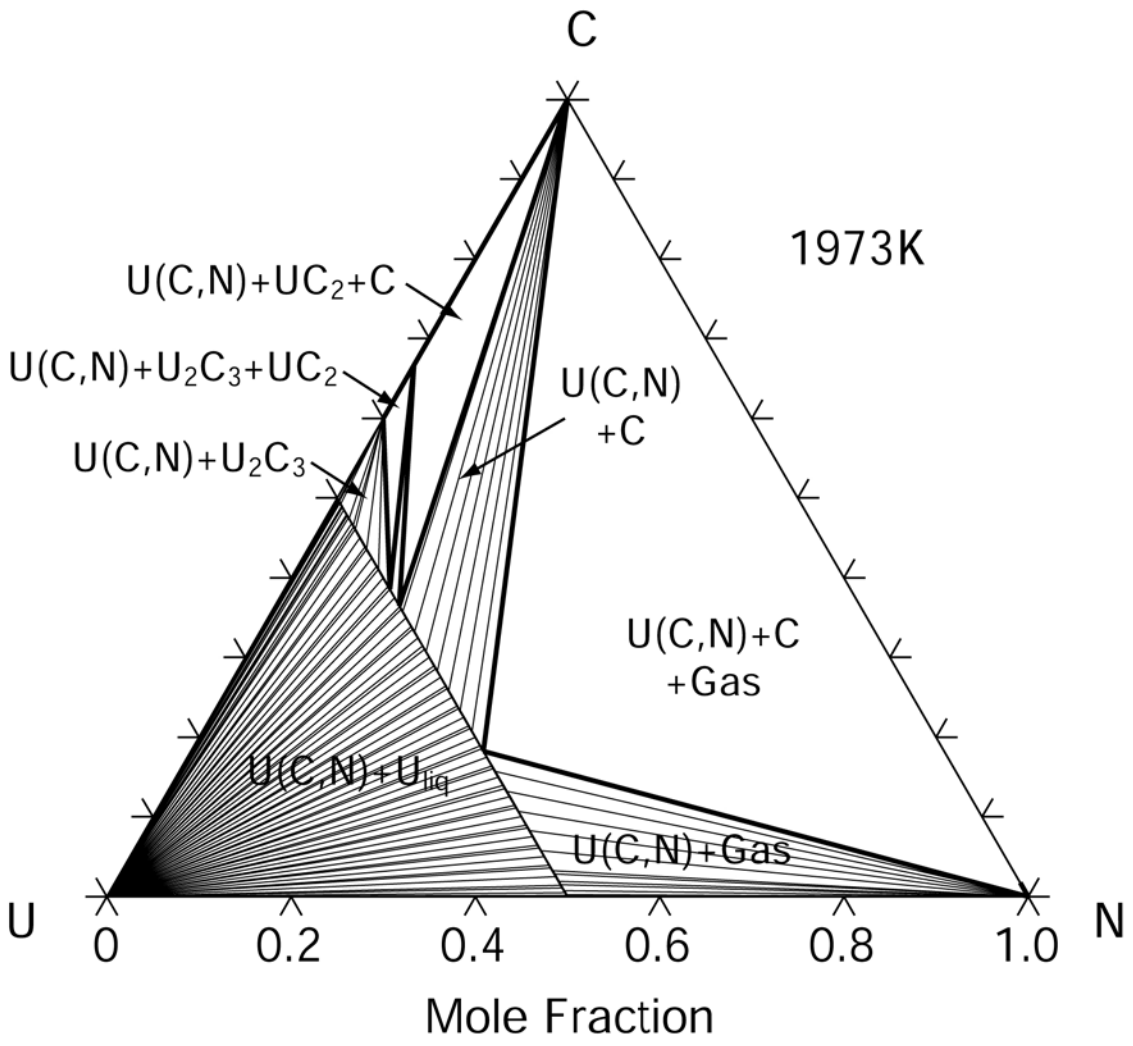

Fig. 5. Computed 1973K phase U-C-N diagram for 1 bar total pressure which exhibits reasonably good agreement with that experimentally determined by Henry and Blickensderfer [6] and estimated by Leitnaker et al. [10].

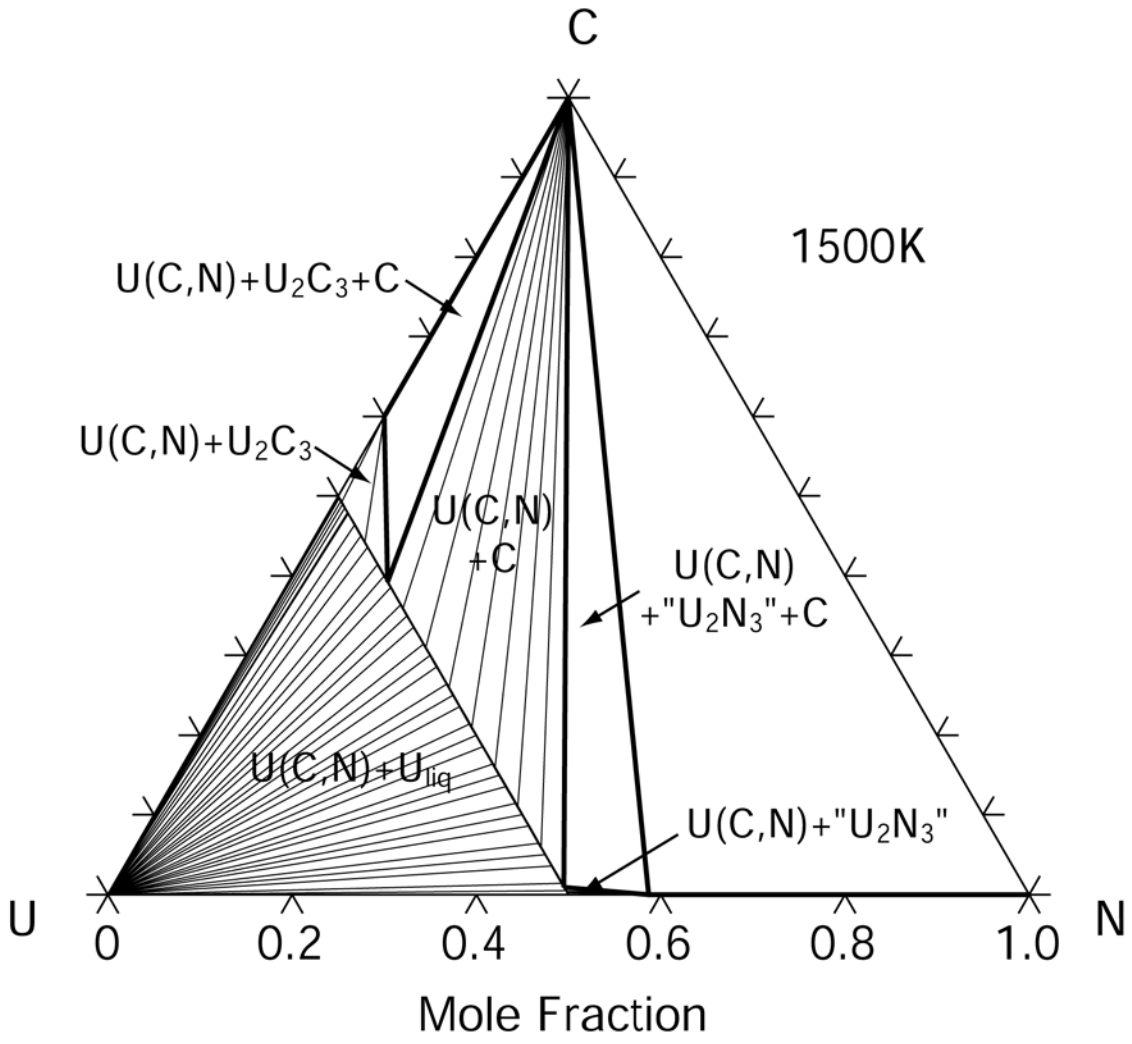

Fig. 6. Computed U-C-N phase diagram at 1500K and 1 bar total pressure illustrating increasing width of U(C,N)-C region with decreasing temperature and the disappearance of the UC_2 phase.

Computed Nitrogen Pressures

In support of fuel processing efforts, values of nitrogen pressure as a function of temperature and composition were computed for the $UC_{1-x}N_x$ phase in equilibrium with either carbon or carbides. The results are provided in Figs. 7 and 8, and in the expressions below. For the equilibria in the phase region of $UC_{1-x}N_x$ with carbon (graphite) the nitrogen pressure is defined by the reaction

$$2[UN]_{UC} + 2C = 2[UC]_{UN} + N_2 \qquad (5)$$

with the free energy change of

$$G_{rxn} = 3.82400E+05 - 219.794\,T + 4.40521\,T\ln(T) + 1.02422E-03\,T^2 + 2.64683E-07\,T^3 -$$

2.51060E+06 T^{-1} + 5.28600E+08 T^{-2}-2.40000E+10 T^{-3}(J/mol). (6)

The resulting expression for the equilibrium nitrogen pressure from the reaction of Eq. 5 and the ideal solution relations of Eq. 1 is

$$pN_2 = \frac{x^2}{(1-x)^2} e^{-G_{rxn}/RT} \quad (7)$$

Similarly, for the phase region containing the sesquicarbide instead of graphite the equilibria defining the nitrogen pressure is

$$2[UN]_{UC} + 2U_2C_3 = 6[UC]_{UN} + N_2 \quad (8)$$

with the free energy change of

G_{rxn} = 3.65542E+05 – 255.104 T + 17.8421 T ln (T) - 4.62504E-02 T^2 + 1.13062E-05 T^3 +

1.46719E+06 T^{-1} (J/mol). (9)

The resulting expression for the equilibrium nitrogen pressure from the reaction of Eq. 8 and the ideal solution relations of Eq. 1 is

$$pN_2 = \frac{x^2}{(1-x)^6} e^{-G_{rxn}/RT} \quad (10)$$

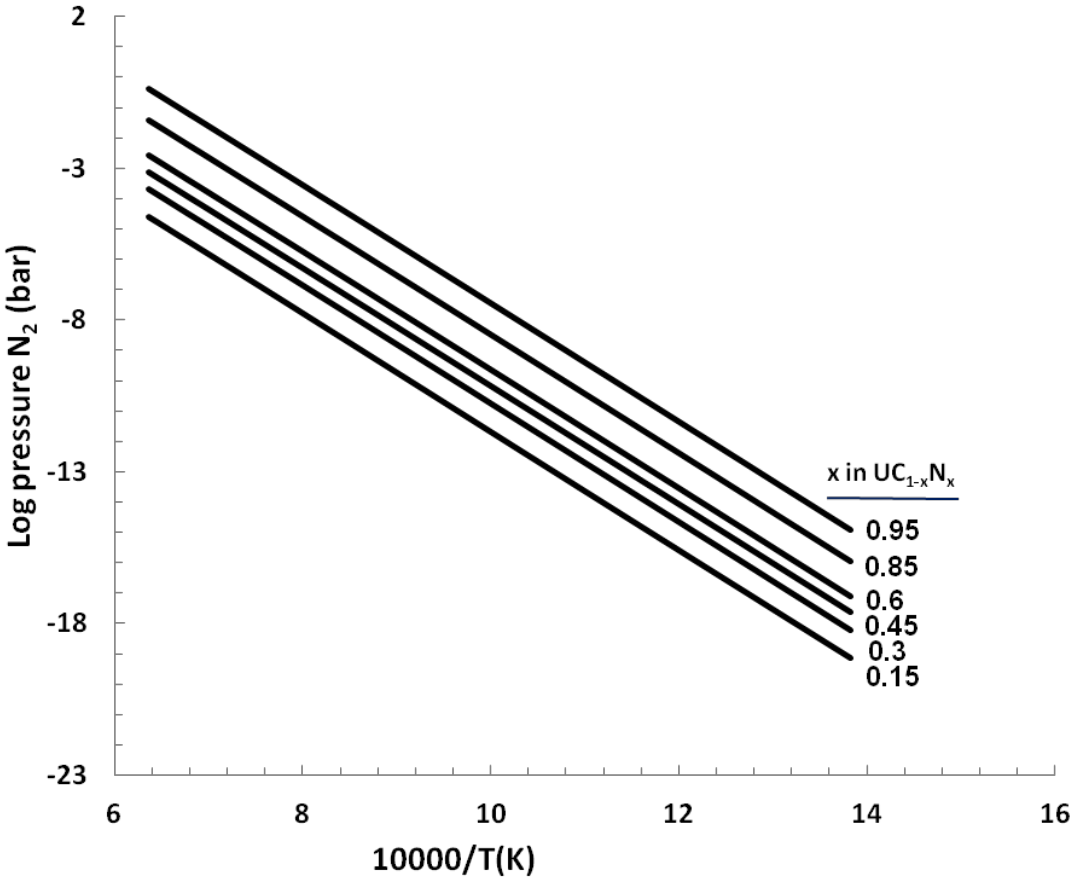

Fig. 7. Computed nitrogen pressure as a function of temperature over 723K-1573K and $UC_{1-x}N_x$ composition in equilibrium with carbon or carbides.

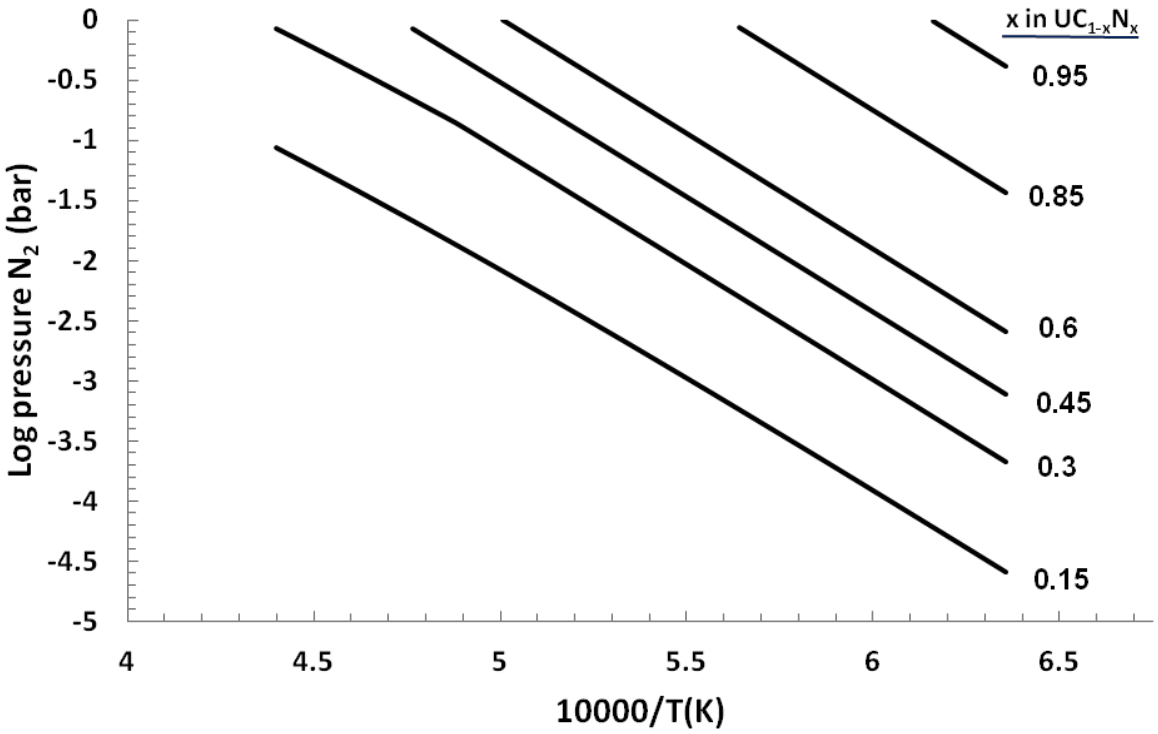

Fig. 8. Computed nitrogen pressure as a function of temperature over 1573K-2273K and $UC_{1-x}N_x$ composition in equilibrium with carbon or carbides.

Implications of U-C-N Representation

Agreement between measured and computed nitrogen pressures in the U(C,N)-U_{liq}, are good provided adjustment is made to the free energy for UN, with the exception of the lowest nitrogen content compositions,. The inability of an ideal solution model to well reproduce the nitrogen pressures reported by Naoumidis and Stoecker [22] for compositions of $UC_{1-x}N_x$ on the high carbon side of the diagram may be due to the multiple second phases that can be in equilibrium with the solution phase, yet which are not reported with the pressure measurements. The phase diagram computed in this work and also determined by Henry and Blickensderfer [6] and Leitnaker et al. [9] show regions at the high temperatures of the data of Naoumidis and Stoecker [22] that include $UC_{1-x}N_x$ with U_2C_3, UC_2, carbon, or nitrogen. Yet the reported pressures as a function of composition do not indicate transitions between phase regions, thus not making it possible to assess in what phase region the measurements were performed. In addition, Katsura et al. [24] note that the amorphous nature of the carbon formed by the reaction of UC with nitrogen in these studies, the extent of which they indicate varies with temperature, may be the cause of the inconsistent results.

The computed phase diagram at 1973K agrees reasonably with that derived from the phase equilibria observations in Henry and Blickensderfer [6] and that estimated by Leitnaker et al. [9]. Henry and Blickensderfer [6], however, indicate U_2N_3 stable at 1973K yet it has been shown to not exist above ~1600K [13].

A wide variety of reports discuss determined activities of UC and UN in the solid solution U(C,N) phase and some resultant regular solution interaction energies.[3-5, 8, 9, 11, 25-28] Ikeda et al. [8] has reviewed purported interaction energies between the carbon and nitrogen atoms on the anion lattice (which, based on their relation, when multiplied by 6 provide interaction energies) and found they vary with temperature from slightly negative to significantly positive. However, in the current effort agreement cannot be obtained utilizing a consistent regular solid solution model without adjustment to the effective heat of formation of UN of Chevalier [13]. After adding the necessary +12 kJ/mol to the Gibbs free energy as noted above, the behavior is well reproduced with an ideal solution of UC and UN. It was also shown that obtaining agreement with nitrogen pressure measurements from decomposition of solely UN requires that same adjustment to the Gibbs free energy. Thus the justification for adjusting the values for UN appears reasonable.

There appears to be an inconsistency in the interpretation of UN decomposition to nitrogen and uranium liquid and the measurement of uranium vapor pressure. Ikeda et al. [8] report uranium pressure measurements in addition to nitrogen pressures from their Knudsen effusion mass spectrometry of U(C,N). The values are consistently below those expected in the presence of liquid uranium, which Ikeda et al. [8] indicate to be in equilibrium with $UC_{1-x}N_x$. They also report decreasing uranium pressures with decreasing values of x, which they note they cannot explain. It is likely that as in the case of UN, the U(C,N) phase can be hypostoichiometric, as shown in the proposed phase diagram of Henry and Blickensderfer [6]. Their measurements therefore may have been performed over single-phase U(C,N) exhibiting a significant homogeneity range, with thus less than unit activity for uranium liquid. This does bring into question the assumption of the solid solution phase having $UC_{1-x}N_x$ stoichiometry, and in equilibrium with uranium liquid in some of the calculations above, but given the level of information on the phase currently available a better assumption is not possible.

Thermomechanics

Efforts are underway to improve the utility of the COMSOL Multiphysics model[1] used to assess the reliability of TRISO particles embedded in a SiC matrix. For example, expressions describing the temperature and porosity dependencies of elastic and thermal properties of the UO_2 kernel, the carbon buffer layer, PyC, and SiC layers as well as the SiC matrix were compiled from numerous references and then programmed into the COMSOL model. These data were also published in an EXCEL workbook for easy distribution to interested persons. Validation of the COMSOL model was carried out by comparing predicted stress profiles with those obtained from previous analyses [28, 29] and from existing analytical solutions (when available).

Three specific studies were implemented during this reporting period. First the single particle model (Fig. 9) was used to estimate the survival probability of the SiC barrier layer as a function of pressure, kernel diameter, and PyC buffer layer thickness. In these analyses the buffer layer served only to transmit the pressure without supporting any elastic stresses. The Weibull modulus and scaling parameters were taken as 8 and 400 MPa $mm^{3/m}$, respectively. The later parameter was fairly conservative given that recent biaxial flexural tests of ORNL SiC disks indicated fracture strengths obtained were well above 400 MPa. The results showed that at a fixed applied pressure

[1] ***COMSOL Inc,*** Palo Alto, CA

the probability of survival of the SiC layer decreased with increasing buffer and kernel diameters consistent with trends based on well-established elastic solutions.

Next a multi-particle model (Fig. 10) was created with the initial intent of predicting stresses during thermal transients (startup). The model consisted of 4 particles in which each kernel could become debonded at a user-specified time. The effect of such debonding for Particle #3 which occurred at 3.8 h was to reduce to zero the tensile stress in the SiC barrier layer for that particle (Fig. 11).

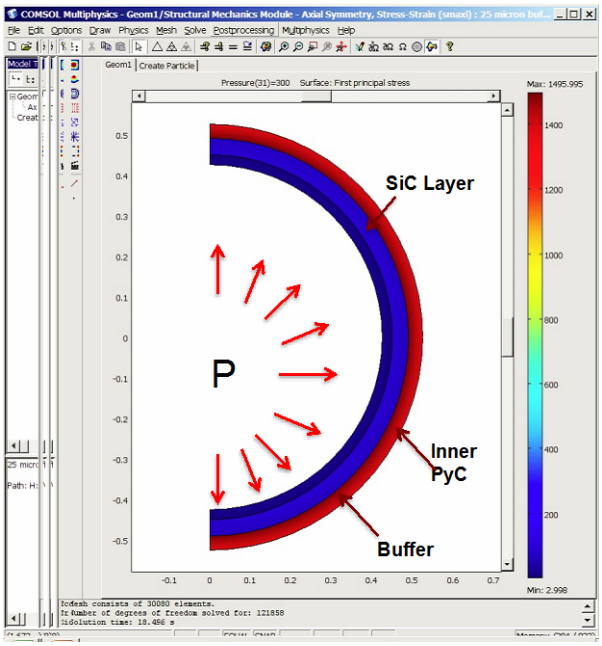

Buffer layer thickness varied from 25 to 100 microns

PyC Layer thickness = 40 microns

SiC Layer thickness = 35 microns

SiC Fracture strength = 400 MPa and Weibull modulus = 8 (1. S.-G. Jong et al. J. Am. Ceram. Soc. 90[1] 184(2007). 2. T. S. Byun et al., Int. J. Appl. Ceram. Technol. 7[3}] 327 (2010)

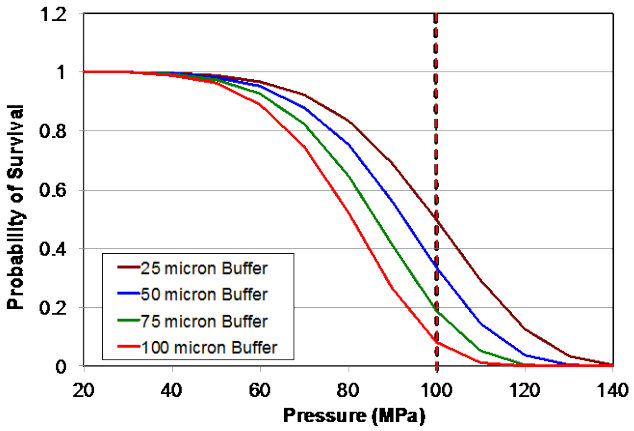

Kernel Diameter = 850 µm

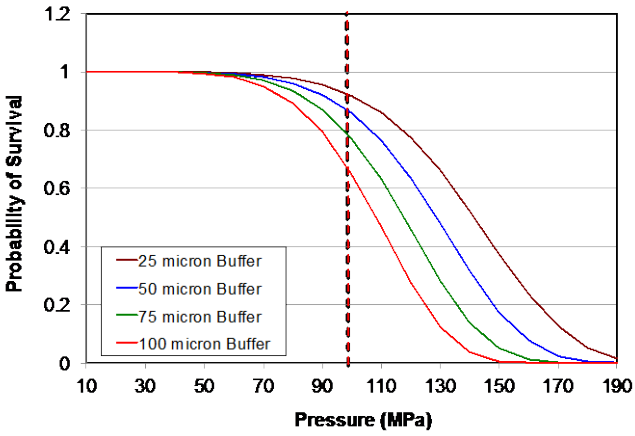

Kernel Diameter = 650 µm

Fig. 9. Predicted probability of survival of SiC barrier layer as a function of the PyC buffer layer thickness and the kernel diameter.

- **Simple 2D Section Considered**
  - No Creep or Swelling
  - No Internal Pressurization
- **Elastic and Thermal Properties Were Prescribed as Functions of Temperature, Porosity, and Fluence**
- **Volumetric Heating Rate of 450 W/cc Assumed**
- **Stresses Calculated With and Without Temperature Gradient**

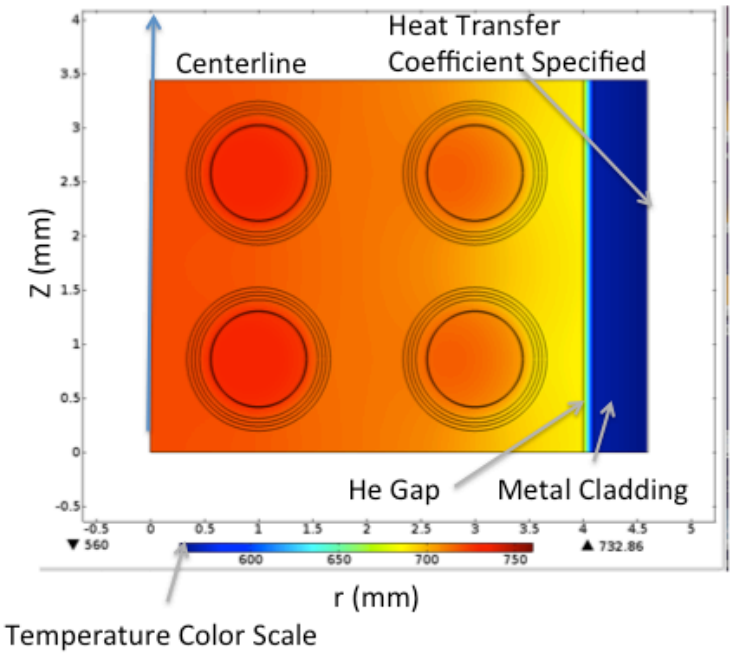

Fig. 10. Four TRISO particle model used to examine stresses generated during transients conditions.

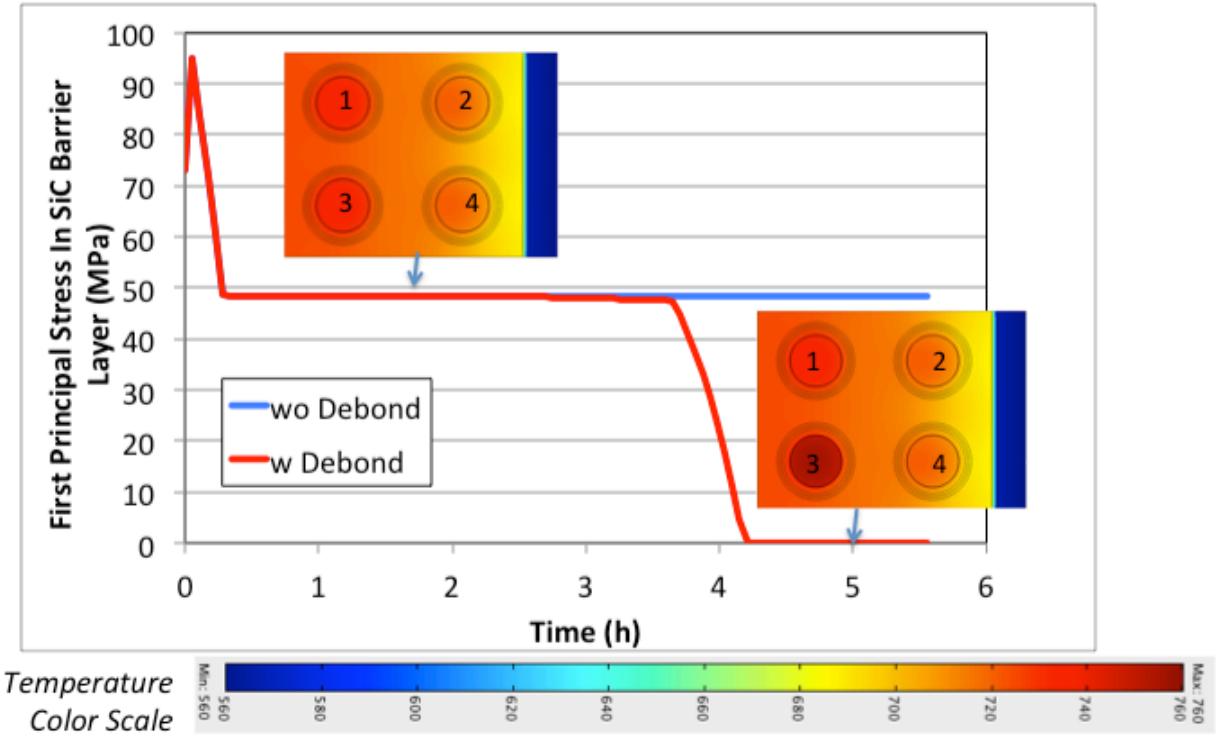

Fig. 11 Stresses generated within TRISO particles during transient conditions with and without debonding of particle 3.

The models described above were based on the assumption of 1) uniform particle sizes and 2) a simple geometric arrangement of particles within the matrix. These limitations in part resulted from the limited solid modeling capability of the COMSOL Multiphysics software used in 2011 and early 2012 (version 3.5a). The current version in use (4.2a), which has a significantly improved interface for building 2D and 3D models, was recently used to create an 8 particle model where the dimensions and locations of each particle within the matrix was determined by a user specified tabular input table. An example of the first principal stress distributions generated for a variable particle size and spacing is shown in Fig. 12. The stress data will subsequently be used to estimate the survival probability of the SiC barrier layer and SiC matrix.

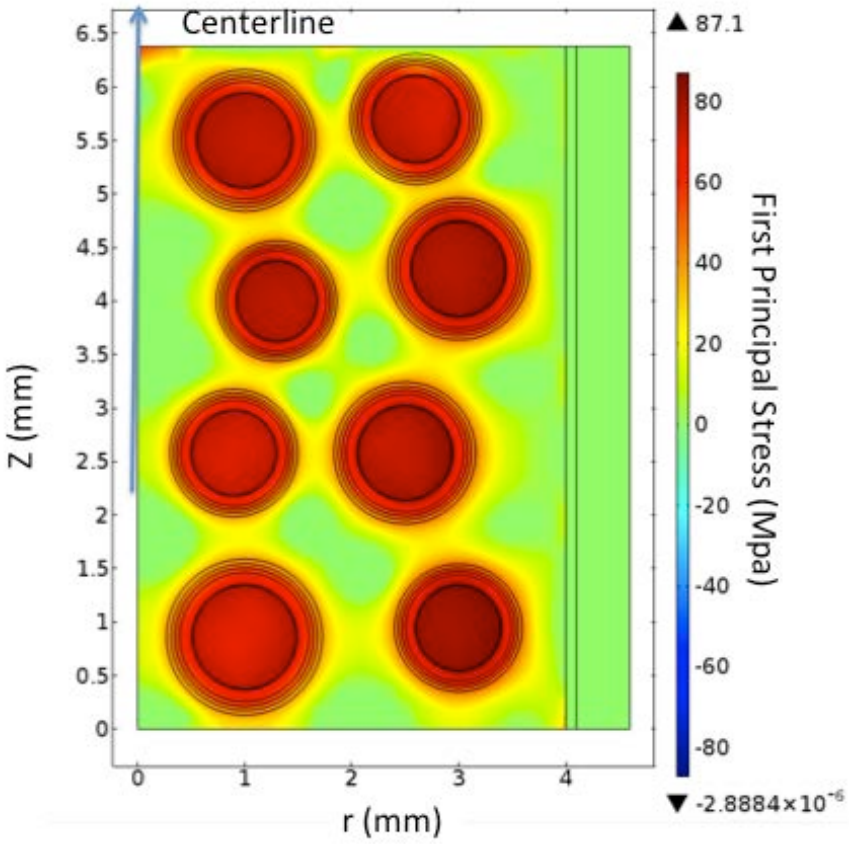

Fig. 12. Example of the predicted distribution of stresses for systems where size and spacing of TRISO particles were varied based on a new model.

Experimental Studies

The thermal conductivities of two ORNL SiC samples P187 A1 and A2 are shown below and compared to those of two commercial SiC ceramics: NC203 that employs alumina as the sintering additive and Hexalloy where boron and carbon additions are used, as well as the early SiC sample prepared at Kyoto University, Fig. 13. Note that while the range of values increases below 600K (e.g., 80 - 120 W/m/K), the conductivities of each of the above samples merge above 600K. The much lower density of sample 11-1633 is a major factor in its much lower conductivity. The P187

samples have densities of 93 and 95% T.D., as compared to ≥98% for the Kyoto and the two commercial SiC samples. This simply highlights the influence of porosity in reducing the conductivities, especially at lower temperatures.

Biaxial fracture strengths were obtained for these same two ORNL SiC ceramics using a ball-on-ring loading configuration with the maximum tensile stress imposed at the center of 1 mm thick disks. The two materials each exhibited fracture strengths in excess of 400 MPa with the higher density sample (P187 A2) having strengths in excess of 600 MPa, Fig. 14. Additional data will be gathered to provide more rigorous input for the modeling studies.

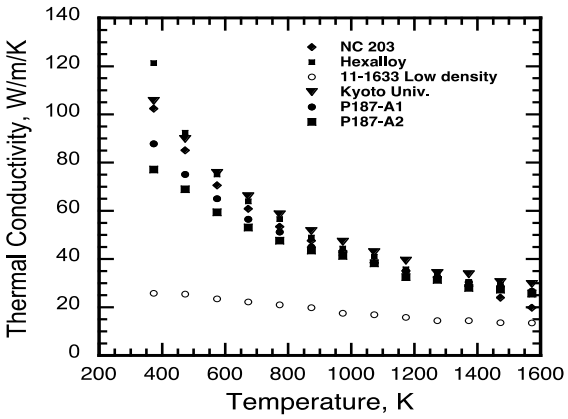

Fig. 13. Thermal conductivities of several SiC ceramics.

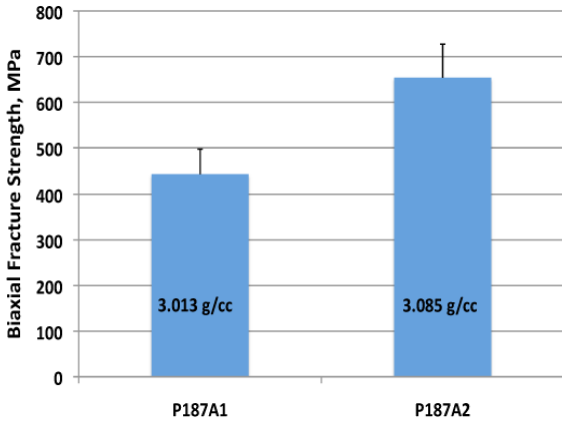

Fig. 14. Fracture strengths of recent ORNL SiC matrix samples.

Future Efforts

The next period will see efforts focusing on continued support of fuel processing and fabrication. These include describing the kinetics of carbothermic reduction/nitridation and the relationships to the final composition of the nitride kernels. Work will also be directed toward understanding phase relations within the particle during burnup with nitrogen release and reaction with bred fission products. The attack on particle layers by silver will be addressed, with research on release mechanisms and rates, and interactions with silicon carbide.

The 8 particle model will be used to examine the role of particle size variability and spacing upon the thermal and stress profiles developed in the fuel rod. The effects of swelling and creep of the PyC layers will be introduced into the model. The underlying physics will be based on the analyses described in Ref [29]. Work will continue to access the strength and thermal conductivity of the SiC matrices as a function of additive compositions and microstructure. Studies will continue on recently initiated characterization of the interfacial properties of cubic zirconia rods with the TRISO coatings utilizing both free standing coated rods and coated rods embedded in the SiC matrix.

Publications

T. M. Besmann, D. Shin, T. B. Lindemer, ”Uranium Nitride as LWR TRISO Fuel: Thermodynamic Modeling of U-C-N,” *J. Nucl. Mater.* 427 (2012), pp. 162-168.

T. M. Besmann, R. E. Stoller, G. Samolyuk, P. C Schuck, S.I. Golubov, S. P. Rudin, J. M. Wills, J. D. Coe, B. D. Wirth, S. Kim, D. D. Morgan, I. Szlufarska, “Modeling Deep Burn TRISO Particle Nuclear Fuel,” *J. Nucl. Mater.* In press. (Note: This paper was submitted for the proceedings of the 2010 ANS summer meeting.)

M. K. Ferber, P. F. Becher, A. A. Wereszczak, and H. T. Lin, “Thermomechanics and Failure Probability of TRISO FCM Fuel,” in preparation.

References

[1] K.A. Terrani, L.L. Snead, J.C. Gehin, "Microencapsulated Fuel Technology for Commercial Light Water and Advanced Reactor Applications,” J. Nucl Mater., submitted.
[2] K.A. Terrani, J.O. Kiggans, Y. Katoh, K. Shimoda, F.C. Montgomery, B.L. Armstrong, C.M. Parish, T. Hinoki, J.D. Hunn, L.L. Snead, “Fabrication and Characterization of Fully Ceramic Microencapsulated Fuels,” J. Nucl. Mater., in press
[3] A.E. Austin and A.F. Gerds, The Uranium-Nitrogen-Carbon System, BMI-1272 (1958).
[4] J.M. Leitnaker, *Thermodynamics of Nuclear Materials, 1967*, IAEA, 1968, p. 317.
[5] T. Sano, M. Katsura and H. Kai, *Thermodynamics of Nuclear Materials, 1967*, IAEA, 1968, p. 301.
[6] J.L. Henry and R. Blickensderfer, J. Amer. Cer. Soc. 52 (1969) 534.
[7] A. Naomidis, J. Nucl. Mater. 34 (1970) 230.
[8] Y. Ikeda, M. Tamaki and G. Matsumoto, J. Nucl. Mater. 59 (1976) 103.
[9] E.H.P. Cordfunke and W. Ouweltjes, J. Nucl. Mater. 79 (1979) 271.
[10] J. M. Leitnaker, T. B. Lindemer, and C. M. Fitzpatrick, J. Am. Ceram. Soc. 53 (1970) 479.
[11] G. Prins and E.H.P. Cordunke, J. Nucl. Mater. 89 (1980) 221.
[12] P.Y. Chevalier and E. Fischer, J. Nucl. Mater. 288 (2001) 100.
[13] P.Y. Chevalier, E. Fischer and B. Cheynet, J. Nucl. Mater. 280 (2000) 136.
[14] C.W. Bale, P. Chartran, S.A. Degterov, G. Eriksson, K. Hack, R.B. Mahfoud, J. Melancon, A.D. Pelton and S. Petersen, FactSage Thermochemical Software and Databases, CALPHAD 26 (2002) 39.
[15] D.R. Stull and H. Prophet, *JANAF Thermochemical Tables*, U.S. Department of Commerce, Washington, (1985).
[16] W. M. Olson and R. N. R. Mulford, J. Phys. Chem. 67 (1963) 952.
[17] P.A. Vozzela and M. A. DeCrescente, *Thermodynamic Properties of Uranium Mononitride*, Pratt and Whitney Aircraft Co., PWAC-479 UNCLAS (1965).
[18] H. Inouye and J. M. Leitnaker, J. Am. Ceram. Soc. 51 [1] (1968) 6.
[19] K. A. Gingerich, J. Chem. Phys. 51 [10] (1969) 4433.
[20] C. A. Alexander, J. S. Ogden, and W. M. Pardue, Trans. Am. Nucl. Soc. 12(1969) 581.
[21] J. Bugl and A. A. Bauer, J. Am. Ceram. Soc. 47 [9] (1964) 425
[22] A. Naoumidis and H.J. Stoecker, *Thermodynamics of Nuclear Materials, 1967*, IAEA, 1968, p. 287.
[23] B. Sundman, B. Jansson, J.O. Andersson, CALPHAD 9 (1985) 153.
[24] M. Katsura, T. Yuki, T. Sano, And Y. Sasaki, J. Nucl. Mater. 39 (1971) 125.

[25] M. Katsura and T. Sano., J. Nucl. Sci. Tech., 3 (1966) 194.
[26] R. Benz, J. Nucl. Mater. 31 (1969) 93.
[27] M. Katsura, A. Naoumidis, and H. Nickel, J. Nucl. Mater. 36 (1970) 169.
[28] M. A. Stawicki, Benchmarking of the MIT High Temperature Gas-Cooled Reactor TRISO-Coated Particle Fuel Performance Model, Submitted To The Department Of Nuclear Science And Engineering In Partial Fulfillment Of The Requirements For The Degrees Of Master Of Science In Nuclear Science And Engineering And Bachelor Of Science In Nuclear Science And Engineering At The Massachusetts Institute Of Technology, May 2006.
[29] G. K. Miller and R. G. Bennett, "Analytical solution for stresses in TRISO-coated particles," Journal of Nuclear Materials 206 (1993) 35-49